



## ADDENDUM TO PROPOSAL P 211

**STUDY OF HIGH ENERGY NUCLEUS-NUCLEUS INTERACTIONS  
WITH THE ENLARGED NA 10 DIMUON SPECTROMETER****EXPERIMENT NA 38**

Annecy<sup>1</sup> - CERN<sup>2</sup> - Clermont-Ferrand<sup>3</sup> - Ecole Polytechnique<sup>4</sup> - Lisbon<sup>5</sup> -  
Lyon<sup>6</sup> - Orsay<sup>7</sup> - Strasbourg<sup>8</sup> - Valencia<sup>9</sup> Collaboration

M.C. Abreu<sup>5</sup>, C. Baglin<sup>1</sup>, A. Baldisseri<sup>1</sup>, A. Baldit<sup>3</sup>, M. Bedjidian<sup>6</sup>, P. Bordalo<sup>5</sup>,  
S. Borenstein<sup>4</sup>, A. Bussi re<sup>1</sup>, P. Busson<sup>4</sup>, R. Cases<sup>9</sup>, J. Castor<sup>3</sup>, C. Charlot<sup>4</sup>,  
B. Chaurand<sup>4</sup>, D. Contardo<sup>6</sup>, O. Drapier<sup>6</sup>, E. Descroix<sup>6</sup>, A. Devaux<sup>3</sup>, J. Fargeix<sup>3</sup>,  
X. Felgeyrolles<sup>3</sup>, R. Ferreira<sup>5</sup>, P. Force<sup>3</sup>, L. Fredj<sup>3</sup>, C. Gerschel<sup>7</sup>, Ph. Gorodetzky<sup>8</sup>,  
P. Gras<sup>9</sup>, B. Grosdidier<sup>8</sup>, J.Y. Grossiord<sup>6</sup>, A. Guichard<sup>6</sup>, J.P. Guillaud<sup>1</sup>, R. Haroutunian<sup>6</sup>,  
D. Jouan<sup>7</sup>, L. Kluberg<sup>4</sup>, R. Kossakowski<sup>1</sup>, G. Landaud<sup>3</sup>, P. Liaud<sup>1</sup>, C. Louren o<sup>5</sup>,  
S. Papillon<sup>7</sup>, L. Peralta<sup>5</sup>, M. Pimenta<sup>5</sup>, J.R. Pizzi<sup>6</sup>, C. Racca<sup>8</sup>, S. Ramos<sup>5</sup>, A. Romana<sup>4</sup>,  
X. Tarrago<sup>7</sup>, R. Salmeron<sup>4</sup>, S. Silva<sup>5</sup>, P. Sonderegger<sup>2</sup>, F. Staley<sup>1</sup>, J. Varela<sup>5</sup>, F. Vazeille<sup>3</sup>

SPOKESMAN: L. KLUBERG  
CONTACTMAN: P. SONDEREGGER

- 
- 1 LAPP, CNRS-IN2P3, Annecy-le-Vieux, France.
  - 2 CERN, Geneva, Switzerland.
  - 3 I.P.C., Univ. de Clermont-Ferrand and CNRS-IN2P3, France.
  - 4 IPNHE, Ecole Polytechnique and CNRS-IN2P3, Palaiseau, France.
  - 5 I.J.P., Lisbon, Portugal.
  - 6 IPN, Univ. de Lyon and CNRS-IN2P3, Villeurbanne, France.
  - 7 IPN, Univ. de Paris-Sud and CNRS-IN2P3, Orsay, France.
  - 8 CRN, CNRS-IN2P3 and Univ. Louis Pasteur, Strasbourg, France.
  - 9 IFIC, Burjasot, Valencia, Spain.

This addendum answers to the specific questions that were raised by our request for the extension of NA 38, as presented in our previous note to the SPSC [1]. The set-up – calorimeter proposed for this extension as well as the quantitative improvements expected from the new data are discussed in detail.

## I. THE GOAL OF NA 38 SECOND PHASE

As pointed out in our “Addendum to Proposal P211” submitted to the SPSC [1], the results of the exploratory phase of experiment NA38 carried out in 1986 and 1987 need more and better data. The observed transverse energy  $E_T$  dependences of

- a) the ratio of  $J/\Psi$ 's to the muon pairs in the mass continuum
- b) the transverse momentum  $P_T$  of the  $J/\Psi$

have triggered a great theoretical effort [2] with the aim of explaining the experimental results [3]. The second phase of experiment NA38 is intended to try and discriminate between the two lines of theoretical models which lead to different predictions (fig. 1), i.e., absorption by nuclear matter or by a dense hadron gas versus Debye colour screening in a quark-gluon plasma.

Our goal is therefore to accumulate a substantially larger amount of data under better experimental conditions. The considered improvements result eventually from a compromise between three different options that cannot be optimized simultaneously, i.e., the quality of the measurement of the transverse energy, the mass resolution of the muon pairs and finally the reduction of the background due to muonic decays of hadrons.

## II. THE EXPERIMENTAL STRATEGY

Our final choice has been determined by the data analysed so far. They show that, for the study of the  $J/\Psi$  and  $\Psi'$  as a function of  $E_T$ , the improvement of the energy measurement and of the mass resolution of the muon pairs bring marginal qualitative gains whereas the reduction of the background will decrease both the statistical errors and the systematic uncertainties which could originate from the

background subtraction. Let us remind here that in the case of Sulphur-Uranium interactions and for muon pair masses of  $1.7 \text{ GeV}/c^2$  for example, about 75 out of 100 opposite sign muon pairs are due to hadronic decays with the set-up used until now, schematically represented on Fig. 2. New data with a significantly lower background are therefore a must although consistent checks indicate that it is extremely unlikely that the results obtained so far are due to an incorrect background subtraction [3].

In order to reduce the background, larger quantities of high density materials, with low  $Z$  to preserve mass resolution, have to be used as absorbers as close to the target as possible. This constraint has led us to consider in our last Addendum [1] two calorimeter-absorber configurations which had been studied and simulated (see Appendix 1 for details). They are discussed hereafter.

### III. THE CU CALORIMETER

The idea was to use a converter with a ratio (interaction length)/(radiation length) smaller than that of Pb so that the calorimeter is, by itself, a more efficient absorber than the present Pb – Fiber calorimeter. The configuration which has been studied (Set-up nr. 1 of Fig. 2) consists of a calorimeter similar to the existing one but using Cu instead of Pb as converter. It is also somewhat shorter, i.e. 8 instead of the present 14 radiation lengths. The calorimeter is separated from the target by 15 cm of BeO and followed downstream by a pure C absorber. With respect to the configuration used in the past and taken as reference, this set-up leads to a somewhat better mass resolution due to multiple scattering ( $\approx 75 \text{ MeV}/c^2$ ) and to a rate of decay muon pairs multiplied by 0.65. A further reduction of the background can be obtained by using a 10 radiation lengths calorimeter followed downstream by a 10 cm thick pure Cu absorber, replacing 10 cm of pure carbon. Background is then multiplied by 0.53 but mass resolution due to multiple scattering rises to the present value of  $90 \text{ MeV}/c^2$ .

The resolution of such a calorimeter for the neutral energy produced at the “knee” of the  $^{32}\text{S}$  spectrum, i.e. for  $170 \pi^0$ 's in the average, is 6.5%, comparable to the resolution of our presently existing calorimeter. Its disadvantage lies in the fact that, together with the neutral energy, it measures about twice the fraction of the charged energy measured previously, i.e. 40% versus 17%. This charged energy is measured with a poor resolution in our electromagnetic calorimeter inducing thus an extra uncertainty which needs a model-dependent correction.

A further disadvantage of this Cu calorimeter is that it needs a new research program for the development of a specific technology.

#### IV. THE "SAMPLING" CALORIMETER

The idea here was to try and separate completely the energy measurement device from the absorbers, so as to decouple the two conflicting requirements of having dense but low  $Z$  material in front of the target and high  $Z$  converter in the calorimeter. This is achieved with the "sampling" calorimeter which occupies only angular domains outside the six circular sectors corresponding to the air gaps of the magnet [1], i.e., outside the useful azimuthal acceptance of the muons in the spectrometer.

In an ideal configuration where absorbers along the trajectories of the accepted muons consist of 100 cm of BeO followed by 445 cm of C as schematically represented by set-up nr. 2 of Fig. 2, it becomes possible to improve the mass resolution due to multiple scattering to  $60 \text{ MeV}/c^2$  instead of the present  $90 \text{ MeV}/c^2$ , with a resulting  $\sigma_{\Psi}$  of  $125 \text{ MeV}/c^2$ . At the same time, the background is multiplied by 0.58.

The linear dimensions of some of the cells of the sampling calorimeter as well as those of the inner rings ( $4.0 < \eta < 5.2$ ) are comparable to those of the developing electromagnetic shower. This would normally lead to a bad resolution for the measurement of the transverse energy in the calorimeter, in particular if the detector was intended to measure the energy of a single particle. As a matter of fact, the proposed experiment measures the flow of neutral energy produced by a large number of photons corresponding typically to about 200  $\pi^0$ 's in the case of central Sulphur-Uranium collisions at 200 GeV/nucleon. As can be easily guessed, the measurement of such a large number of photons minimizes fluctuations. The simulation performed with a Monte-Carlo program (see details in Appendix 1) has been confirmed by a manipulation of our experimental data. It shows that  $\sigma(E_{\perp}^0)/E_{\perp}^0$ , the relative resolution of the neutral transverse energy flow measured in the calorimeter, goes like  $1/\sqrt{N}$ , where  $N$  is the number of detected neutral pions. The "sampling calorimeter" considered here has an overall resolution  $\sigma(E_{\perp}^0)/E_{\perp}^0 \simeq 9.5\%$ , to be compared to 5.5% obtained in the runs of 1986-1987. Moreover this resolution gets even worse and amounts to  $\sigma(E_{\perp}^0)/E_{\perp}^0 \simeq 16\%$  if we con-

sider only the neutral transverse energy measured in the pseudo-rapidity interval corresponding to the muon pairs, i.e.  $2.8 < \eta < 4.0$ , as in this region the calorimeter covers only one third of the azimuthal space. This serious drawback, although tolerable in our case, has nevertheless led us to a different choice, as detailed hereafter.

## V. THE PROPOSED SET-UP

The performances of the set-up built with the Cu calorimeter have been studied in detail. They are in fact similar to those obtained with a set-up in which the present 14 radiation lengths Pb-Fiber calorimeter is replaced by an identical but thinner one, with only 8.2 radiation lengths. This calorimeter is separated from the target by 15 cm of BeO followed by 2 cm of Cu, a total of 2.5 radiation lengths which approximately places the maximum of the shower energy around the middle of the Pb converter of the calorimeter. The reading system behind it is replaced by a much more compact one leaving only the equivalent of 5 cm of air (to be compared with 15 cm presently). It is followed by a 12 cm long Cu absorber. This configuration is represented by set-up nr. 3 of Fig. 2. With this set-up and contrary to the Cu calorimeter idea, the energy measurement and the absorber function are again separated but, with this optimized configuration :

- a) The quality of the neutral transverse energy measurement is preserved with  $\sigma(E_T^0)/E_T^0 \simeq 6\%$  despite the shorter length and because of the large number of showers measured in each cell, which minimizes fluctuations.
- b) The muon pair mass resolution due to multiple scattering stays the same, i.e.  $\simeq 90 \text{ MeV}/c^2$  and
- c) background is multiplied by 0.49 with respect to the configuration used in the past.

## VI. ADVANTAGES OF THE PROPOSED SET-UP

We feel it is absolutely necessary to keep at least the same transverse energy resolution as in the past, as transverse energy is the critical physical parameter governing the new effects that we have

observed. This is the reason that makes us put aside the proposed "sampling" calorimeter and adopt, finally, this much more conservative solution.

It should be pointed out that, concerning the muon pair mass resolution and the background, the performances of the proposed set-up are identical to those of the Cu calorimeter, provided that the 12 cm long Cu absorber located downstream of the calorimeter are replaced by Carbon. Nevertheless we prefer to favour the reduction of background and make use of this Cu absorber. Concerning the energy measurement, the proposed set-up measures the neutral energy together with 25% of the charged energy whereas the Cu calorimeter measures a significantly higher amount of the charged energy, i.e. 40%, with big fluctuations on an event by event basis.

Finally, another advantage of sticking to the Pb-Fiber calorimeter is to stay within a line of detector the technology of which is presently being improved [4]. We intend to use a net of 1 mm diameter stainless steel pipes, with a 50  $\mu$  thick wall, imbedded in a Pb structure, with a Pb to Fiber volume ratio of 2:1. The 1 mm diameter scintillating fibers are simply slipped into the pipes without being glued which, according to present experience [5] improves significantly resistance to radiation damage. Moreover, damaged fibers, can very easily be replaced, if necessary, in the most exposed central region of the calorimeter which contains about 500 fibers (out of a total of 16000 fibers). The reading system will use the same number of (non-scintillating) fibers as the calorimeter itself, allowing thus, for simple reasons of space and curvature constraints, a much more compact system than in our present detector.

Fig. 2 gives the description of the different set-ups considered here and Table 1 their detailed performances. Fig. 3 shows the corresponding mass resolutions as a function of the mass of the muon pair.

## VII. THE PHYSICS PROGRAM FOR 1990 : A SENSITIVITY STUDY

In order to achieve the goal presented in section I, we need to increase significantly the statistics with the Sulphur beam to be able to :

1. Improve the accuracy for the  $J/\psi$  to Continuum ratio and its  $P_T$  dependence.
2. Measure more accurately the  $P_T$  dependence of the muon pairs in the mass continuum.

### 3. Study the behaviour of the $\Psi'$ relative to the $J/\Psi$ .

The experimental accuracy that can be expected from a reasonable period of data taking has been investigated with our present Sulphur-Uranium data using the following method detailed in Appendix 2. The Mass and transverse momentum  $P_T$  spectrum of the muon pairs in the continuum have been parametrized in the mass interval  $1.7 < M < 2.7 \text{ GeV}/c^2$ . The  $P_T$  dependence as well as the experimental mass resolution of the  $J/\Psi$  have also been described analytically. Finally, the observed dependence on the transverse energy  $E_T$  of the ratio  $(J/\Psi)/\text{continuum}$  has been introduced. The background originating mainly from  $\pi$  and K decays has also been parametrized in mass and  $P_T$  in agreement with the observed experimental distributions of like sign muon pairs. Data have then been simulated by mixing "signal" and "background" events randomly chosen according to the parametrized distributions. Taking as reference the signal to background ratio observed in our real data, we are able to change it and, in particular, to simulate a sample of data with a signal to background ratio multiplied by a factor of 2. An analysis identical to the one used for our real data is then applied in order to subtract the background, considered as unknown, and to compute the  $J/\Psi$  to continuum ratio as a function of the measured transverse energy and of the transverse momentum  $P_T$  of the muon pair. Fig. 4 shows the ratio of the  $P_T$  distributions of events with muon pair masses between 2.7 and 3.5  $\text{GeV}/c^2$ , i.e. of  $J/\Psi$ 's, for  $E_T > 137 \text{ GeV}$  and  $P_T < 38 \text{ GeV}$ . The three figures relate to our real experiment, to a simulated experiment with same statistics and same signal/background ratio used as check of the method and to an experiment simulated with 10 times more luminosity than collected in the past, but only half the background/signal ratio. In this last case, the relative error on the ratio  $J/\Psi/\text{continuum}$  integrated over  $P_T$  is multiplied, on the average, by 0.25 with respect to our present results. Fig. 5, similar to fig. 4, shows the corresponding distributions for muon pairs in the mass continuum, i.e. with  $1.7 < M_{\mu\mu} < 2.7 \text{ GeV}/c^2$ . As seen from Fig. 5(b) and 5(c), a significant improvement is expected for the continuum, allowing quantitative conclusions, at least for  $P_T < 2 \text{ GeV}/c$ . Finally, with the proposed experiment and 10 times more luminosity than already collected with incident S, we expect around 1600  $\Psi'$  and 120000  $J/\Psi$ 's. Such a sample of events will lead to an accuracy of about 6% for the ratio  $\Psi'/\Psi$  in each of the six equally populated transverse energy bins. It should allow a comparison with theoretical predictions (fig. 6) and make easier a validity check of the different explanations proposed so far.

## VIII. BEAM TIME REQUEST

In order to be able to make a significant quantitative progress in the understanding of the results obtained during the exploratory runs of 1986 and 1987, we request an extension of experiment NA38.

The goal is :

1. To study experimentally the compactified calorimeter-absorber configuration;
2. To measure the proportion of correlated meson decay pairs in a sulphur beam (by taking data without hadron absorber near the target);
3. To increase our present luminosity by a factor of 10 with improved experimental conditions that will decrease our background by a factor of 2.

This program could be achieved with about 85 days of routine data taking with at least  $3 \cdot 10^7$  200-GeV/nucleon Sulphur ions per burst. It is our understanding that this intensity can be delivered without any problem by the ion source. Prior to our data taking periods with Sulphur beam, short periods of proton beam are also requested in order to test our new calorimeter and tune the entire set-up. The collaboration is financially prepared for the improvements described in this Addendum and could have the new set-up ready nine months after approval of the extension asked for here.



## APPENDIX 1

### MONTE-CARLO SIMULATIONS OF THE ENERGY MEASUREMENT IN THE CALORIMETERS

A Monte-Carlo simulation including GEANT.3 for the description and propagation of the electromagnetic showers has been used for the study of the different calorimeters proposed in this Addendum. In the case of the existing calorimeter, and as a check of the method, the results of the simulation have been compared with the real calibration measurements done with 1.5, 3.5, 5, 10 and 20 GeV electron beams. The agreement between simulations and real measurements concerning linearity, efficiency (calibration factors) and resolution is quite satisfactory. The numbers given hereafter refer to the calorimeter used in the runs of 1986 and 1987 but similar studies have been done for each of the calorimeters considered in the Addendum.

#### I. MEASUREMENT OF A SINGLE SHOWER

The resolution of the measurement is determined by geometrical losses as the dimensions of the smallest elements of the calorimeter are similar to those of an electromagnetic shower. For an electron hitting the center of an element, fluctuations due to geometrical losses are minimized and the intrinsic resolution of the calorimeter is given by  $\sigma_{\text{I}}(E) = 0.3/\sqrt{E}$ . The fluctuations that induce this relatively poor resolution become negligible when a flow of several hundreds of particles are detected and measured simultaneously. No linearity problem is observed between 1.5 and 20 GeV. Finally, the simulation of electrons hitting any point of the calorimeter predicts measurements which are in excellent agreement with those obtained with a real beam hitting the corresponding points. This indicates that the geometrical effects are correctly described in the model.

## II. MEASUREMENT OF A FLOW OF NEUTRAL PIONS

The experimental situation has been simulated with a generated flow of  $N$  neutral pions, corresponding to Sulphur interactions with a heavy target.

a/ The rapidity distribution  $dN/d\eta$  has been taken from the experimental results of NA34 [6].

b/ The transverse momentum distribution has been parametrized according to the experimental results by  $dN/dP_T = P_T \times \text{Exp}(-P_T/T_0)$  with  $T_0 = 200$  MeV.

Each particle of energy  $E_i$  is propagated with GEANT.3 through the different materials, subtargets, absorbers and calorimeter.  $E'_i$  is the energy measured in the calorimeter. For a given ring of the calorimeter, hit by  $n$  particles, the measured energy is

$$E_{\text{meas}} = 1/\bar{\varepsilon} \sum E'_i$$

with  $\bar{\varepsilon}$  determined for each individual ring by the calibration run. The energy resolution is then given by the width of the distribution of

$$\Delta E = \sum E_i - 1/\bar{\varepsilon} \sum E'_i$$

with  $\langle \Delta E \rangle = 0$  (no energy bias). A similar procedure is applied for each one of the rings of the calorimeter and leads, for a central Sulphur-Uranium interaction with 200  $\pi^0$ 's in the rapidity interval ( 1.0 , 5.0 ), to a neutral transverse energy resolution  $\sigma(E^0_T)/E^0_T = 3.0\%$ . This resolution goes like  $1/\sqrt{N}$  where  $N$  is the number of detected  $\pi^0$ 's in the calorimeter.

## III. MEASUREMENT OF A FLOW OF NEUTRAL AND CHARGED PIONS

As a matter of fact, the calorimeter is hit by a flow of neutral pions together with twice as many charged pions in the average. A flow of charged pions has also been generated and the corresponding values of  $\varepsilon$  have been computed. In the average  $\bar{\varepsilon}_{\text{charged}} = 0.25 \times \bar{\varepsilon}_{\text{neutral}}$  as seen from Figs. 7 and 8. Finally the combination of neutral and charged pions leads to a neutral transverse energy resolution of 5.5%, to be compared to 3.0% if nature would only produce neutral pions.

## APPENDIX 2

### STUDY OF THE SENSITIVITY OF NA38 WITH THE PROPOSED SET-UP

The purpose of this study is to evaluate the sensitivity of the forthcoming experiment, assuming a total luminosity 10 times higher than already accumulated with a Sulphur beam, during 10 days, at an average intensity of  $1.5 \cdot 10^7$  ions/burst, corresponding to our run of 1987. It is also assumed that the signal/background ratio is increased by a factor of 2 as expected from the calculations performed with the proposed set-up.

#### I. PARAMETRIZATION OF THE DATA

The following phenomenological parametrizations have been used with numerical values deduced from fits to the data already collected with a Sulphur beam.

a/ For muon pairs in the mass continuum between 1.7 and 2.7 GeV/c<sup>2</sup>

$$\frac{dN_c(E_T)}{dM dP_T} (M, P_T) \propto \frac{n_c(E_T)}{M^3} \text{Exp}(-M/M_c) \times P_T \times \text{Exp}(-\pi/4 \times P_T^2 / \langle P_{c,T}^2 \rangle_M)$$

with  $M_c = 1.13 \text{ GeV}/c^2$  and  $\langle P_{c,T}^2 \rangle_M$  given by the following table:

Table 1:

$\langle P_{T}^c \rangle_M$	0.70	0.75	0.80	0.85	0.89	0.93	0.96	1.00	1.03
M	1.75	2.00	2.25	2.50	2.75	3.00	3.25	3.50	3.75

deduced from [7].  $\langle P_{T}^c \rangle_M$  is taken independent of  $E_T$ , as indicated by the data.

**b/ For the J/Ψ**

$$\frac{dN_{J/\Psi}(E_T)}{dM dP_T} (M, P_T) \propto n_{J/\Psi}(E_T) \times \text{Exp}\left(-\frac{(M - M_{J/\Psi})^2}{2\sigma_{J/\Psi}^2}\right) \times P_T \times \text{Exp}\left(-\pi/4 \times P_T^2 / \langle P_{T}^{J/\Psi} \rangle^2 E_T\right)$$

with  $M_{J/\Psi} = 3.097 \text{ GeV}/c^2$ ,  $\sigma_{J/\Psi} = 0.145 \text{ GeV}/c^2$  and

$\langle P_{T}^{J/\Psi} \rangle_{E_T} = 1.077 + 0.95 \cdot 10^{-3} (E_T)$ , with  $E_T$  in  $\text{GeV}/c^2$ , in agreement with our experimental data.

**c/ For the ratio (J/Ψ)/Continuum**

The variation of the ratio (J/Ψ)/Continuum has been smoothed according to:

$$\frac{N_{J/\Psi}(E_T)}{N_c(E_T)} = 13.88 - 0.2717 \times 10^{-1} E_T - 0.9454 \times 10^{-6} (E_T)^2 - 0.1360 \times 10^{-5} (E_T)^3$$

with  $E_T$  in GeV, which leads to the following values in the six  $E_T$  bins used for the analysis of the data:

$E_T(\text{GeV})$	$(J/\Psi)/\text{Continuum (Data)}$	$(J/\Psi)/\text{Continuum (smoothed)}$
38	$13.07 \pm 1.20$	12.77
63	$11.55 \pm 1.10$	11.82
84	$11.24 \pm 1.04$	10.79
101	$8.87 \pm 0.81$	9.72
116	$10.65 \pm 1.11$	8.59
137	$6.54 \pm 0.62$	6.64

d/ For the background, deduced from the like-sign muon pairs

$$\frac{dN_b(E_T)}{dM dP_T} (M, P_T) \propto n_b(E_T) \times \text{Exp}(-\alpha(E_T) \times M) \times P_T \times \text{Exp}(-\pi/4 \times P_T^2 / \langle P_T^2 \rangle_M)$$

with  $\alpha(E_T) = 4.30$  ,  $\langle P_T^2 \rangle_M = 0.205 + 0.321 M$  and  $M$  in  $\text{GeV}/c^2$ .  $n_b(E_T)$  takes into account the sign of the muons and of the magnetic field and satisfies the relations:

$$N_{--^+} / N_{++^+} = 1.0 \text{ for a "positive" field}$$

$$N_{--^-} / N_{++^-} = 0.29 \text{ for a "negative" field}$$

## II. THE SIMULATED SAMPLE OF EVENTS

For each one of the six bins in  $E_T$ , we randomly generate  $N_c$  events in the mass continuum,  $N_\Psi$  events of the type  $J/\Psi$  and two samples of  $N_{--^+}$ ,  $N_{++^+}$ ,  $N_{--^-}$  and  $N_{++^-}$  background events, according to the distributions detailed above. We then simulate, in each  $(M, P_T)$  cell, a sample of opposite-sign muon pair "data events", including background, according to:

$$N_{\mu\mu}(M, P_T) = N_c(M, P_T) + N_\Psi(M, P_T) + 2\sqrt{N_{++^+}} \times N_{--^+} + 2\sqrt{N_{++^-}} \times N_{--^-}$$

using the first sample of generated background events. From these "data events", we then subtract the background, considered as unknown, using the second sample of generated background events and the method applied to our real data, i.e.,

$$N_{\mu\mu}(M, P_{\Gamma}) = N_c(M, P_{\Gamma}) + N_{\Psi}(M, P_{\Gamma}) - 2\sqrt{N_{++} + xN_{--} + -2\sqrt{N_{++} - xN_{--}}}$$

### III. THE RESULTS OF THE ANALYSIS

The events obtained as described above are then analyzed exactly with the same method as our real data.

Taking as reference these real data, we start with a sample of similar size and same signal/background ratio. We find the following results:

$E_{\Gamma}$	$M_c$	(J/Ψ)/Continuum
38	$1.06 \pm 0.07$	$13.56 \pm 1.13$
63	$1.16 \pm 0.08$	$11.15 \pm 0.88$
84	$1.12 \pm 0.07$	$10.89 \pm 0.77$
101	$1.08 \pm 0.07$	$10.52 \pm 0.88$
116	$0.92 \pm 0.06$	$10.44 \pm 0.98$
137	$1.09 \pm 0.07$	$6.69 \pm 0.59$

These results are quite comparable to those obtained with our real data, as could be expected.

Playing the same game again, but with a sample 10 times larger and a signal/background ratio multiplied by 2, leads to the following results:

$E_{\Gamma}$	$M_c$	(J/Ψ)/Continuum
38	$1.15 \pm 0.03$	$12.52 \pm 0.28$
63	$1.10 \pm 0.02$	$12.17 \pm 0.27$
84	$1.12 \pm 0.02$	$10.83 \pm 0.21$
101	$1.14 \pm 0.02$	$9.65 \pm 0.21$
116	$1.09 \pm 0.02$	$8.97 \pm 0.20$
137	$1.15 \pm 0.02$	$6.53 \pm 0.16$

The relative error on the ratio (J/Ψ)/Continuum is thus multiplied by 0.25 in the average.

## REFERENCES

- [1] Addendum to proposal P 211. CERN/SPSC 88-24, SPSC/P 211/ADD 2 (June 1988).
- [2] T. Matsui and H. Satz, *Phys. Lett.* 178B (1986) 416. Published before the beginning of our experiment.
- F. Karsch et al., *Z. Phys. C - Particles and Fields* 37 (1988) 617.
- F. Karsch and R. Petronzio, *Phys. Lett.* 193B (1987) 105.
- F. Karsch and R. Petronzio, *Z. Phys. C - Particles and Fields* 37 (1988) 627.
- J.P. Blaizot and J.Y. Ollitrault, *Phys. Lett.* 199B (1988) 499.
- M.-C. Chu and T. Matsui, *Phys. Rev. D* 37 (1988) 1851.
- C. Gerschel and J. Hüfner, *Phys. Lett.* 207B (1988) 259.
- A. Capella et al., *Phys. Lett.* 206B (1988) 354.
- A. Capella, Proceedings of the 23rd Rencontre de Moriond (1988) ed. by Tran Thanh Van.
- S. Gavin et al., *Phys. Lett.* 207B (1988) 257.
- T. Ftacnik et al., *Phys. Lett.* 207B (1988) 194.
- S. Brodsky et al., Proceedings of the XXIV International Conference On High Energy Physics, Munich, (1988).
- J.-P. Blaizot and J.-Y. Ollitrault, *Phys. Rev. D* 39 (1989) 232.
- [3] C. Baglin et al., The Production of  $J/\psi$  in 200 GeV/nucleon Oxygen-Uranium Interactions, NA38 Collaboration, to be published in *Physics Letters B*.
- P. Sonderegger et al., Proceedings of the XXIV International Conference On High Energy Physics, Munich, (1988).
- P. Bordalo et al., Proceedings of the 23rd Rencontre de Moriond (1988) ed. by Tran Thanh Van.
- A. Romana et al., Proceedings of the International Conference on Physics and Astrophysics of Quark-Gluon Plasma, Bombay, (1988).
- [4] M. Wigmans et al. LAA project.
- [5] P. Sonderegger et al., Radiation damage to scintillating fibers, LIP, Lisbon. Unpublished.

- [6] T. Akesson, Transverse Energy Distributions in Nucleus-Nucleus Collisions, Proceedings of the XXIV International Conference On High Energy Physics, Munich, (1988).
- [7] H. Fritzsch and P. Minkowski, Phys. Lett. 73B (1978) 80.



FIGURE CAPTIONS

**Fig. 1 .** Fraction of remaining  $J/\Psi$ 's, integrated over  $P_T$ , as a function of the number of participants, after suppression by a quark-gluon plasma (top) or absorption by a pion gas (bottom). From J.P. Blaizot and J.Y. Ollitrault, Phys. Rev. D39 (1989) 232.

**Fig. 2 .** Schematic lay-outs of the different set-ups. The number of interaction and radiation lengths are indicated for each block of material within 75 cm from the center of the target. See Table I.

**Fig. 3 .** Mass resolution of the muon pairs for the different set-ups.

**Fig. 4 .** Ratio of the  $P_T$  distributions of muon pairs with mass between 2.7 and 3.5  $\text{GeV}/c^2$  for  $E_T > 125 \text{ GeV}$  and  $E_T < 51 \text{ GeV}$ .

**Fig. 5 .** Ratio of the  $P_T$  distributions of muon pairs with mass between 1.7 and 2.7  $\text{GeV}/c^2$  for  $E_T > 125 \text{ GeV}$  and  $E_T < 51 \text{ GeV}$ .

**Fig. 6 .** Comparison of the  $P_T$  dependence of the  $J/\Psi$  and  $\Psi'$  suppression rates. From F. Karsch and R. Petronzio, *Z. Phys. C - Particles and Fields* 37 (1988) 627.

**Fig. 7 .** Fraction of energy measured by each one of the 5 rings of the calorimeter as a function of the rapidity of the photon.

**Fig. 8 .** Same as Fig. 7 for charged particles.

**Table 1 .** Characteristics of the different set-ups.

	Transverse neutral Energy resolution		Mass resolution (MeV/c <sup>2</sup> )		Signal/Background ratio for a mass of				L/λ <sub>R</sub> for z < 75 cm	L/λ <sub>i</sub> for z < 75 cm	Fraction of the charged energy in E <sub>T</sub> <sup>meas</sup>
	1.7 < η < 4.2	2.8 < η < 4.0	σ <sub>φ</sub>	σ <sub>ψ</sub>	1.0 GeV/c <sup>2</sup>	1.7 GeV/c <sup>2</sup>	2.2 GeV/c <sup>2</sup>	3.1 GeV/c <sup>2</sup>			
S	5.5 %	7.8 %	89	142	0.44	0.33	0.85	∞	15.9	1.05	26 %
E	7.5 %	10.8 %	75	133	0.68	0.51	1.31	∞	9.7	1.35	40 %
T	9.5 %	16.0 %	60	125	0.76	0.57	1.47	∞	4.1	1.60	14 %
U	6.0 %	8.4 %	92	143	0.90	0.67	1.73	∞	20.2	2.00	25 %
P	6.0 %	8.4 %	80	136	0.72	0.54	1.39	∞	12.4	1.45	25 %

Table 1

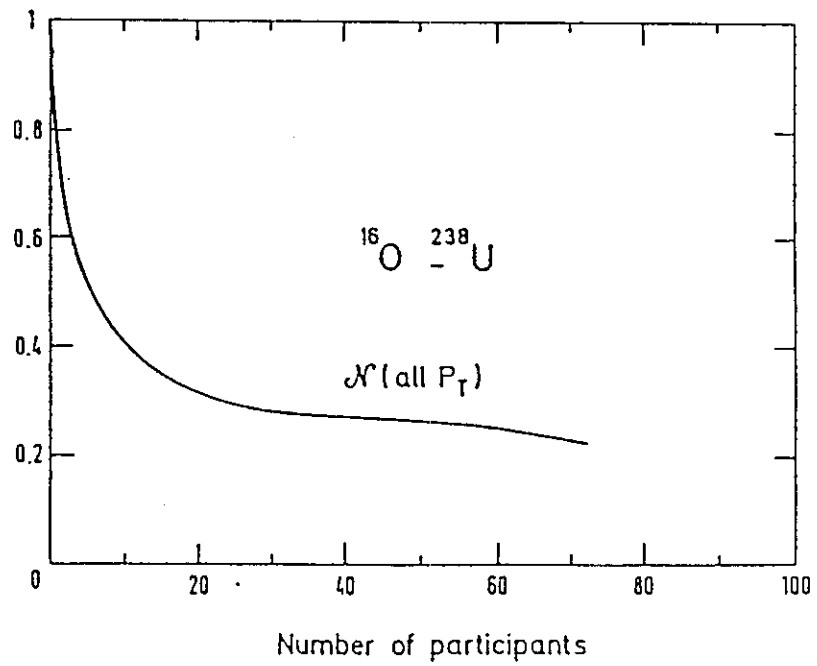
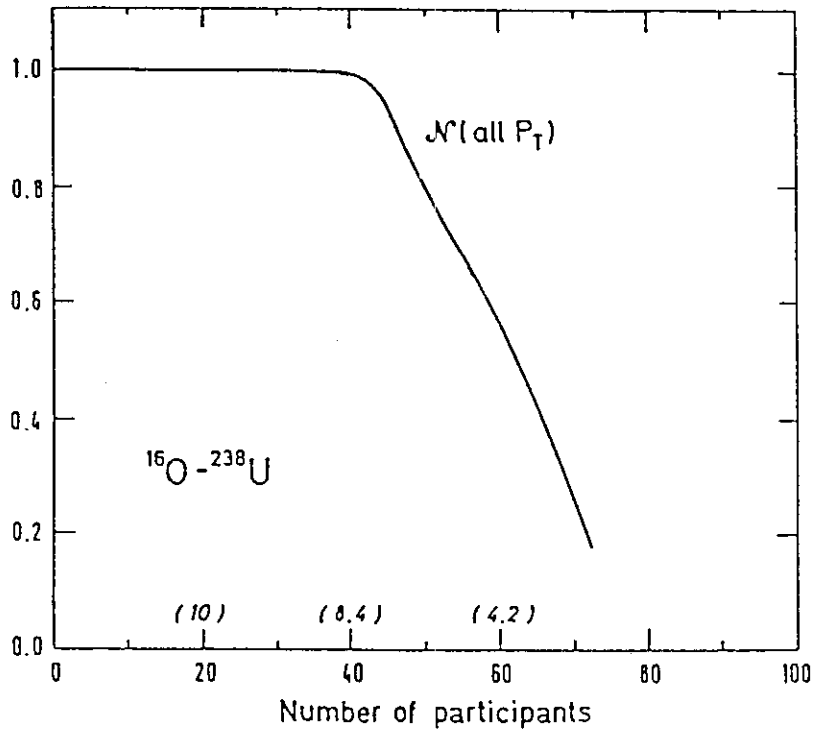


Fig. 1

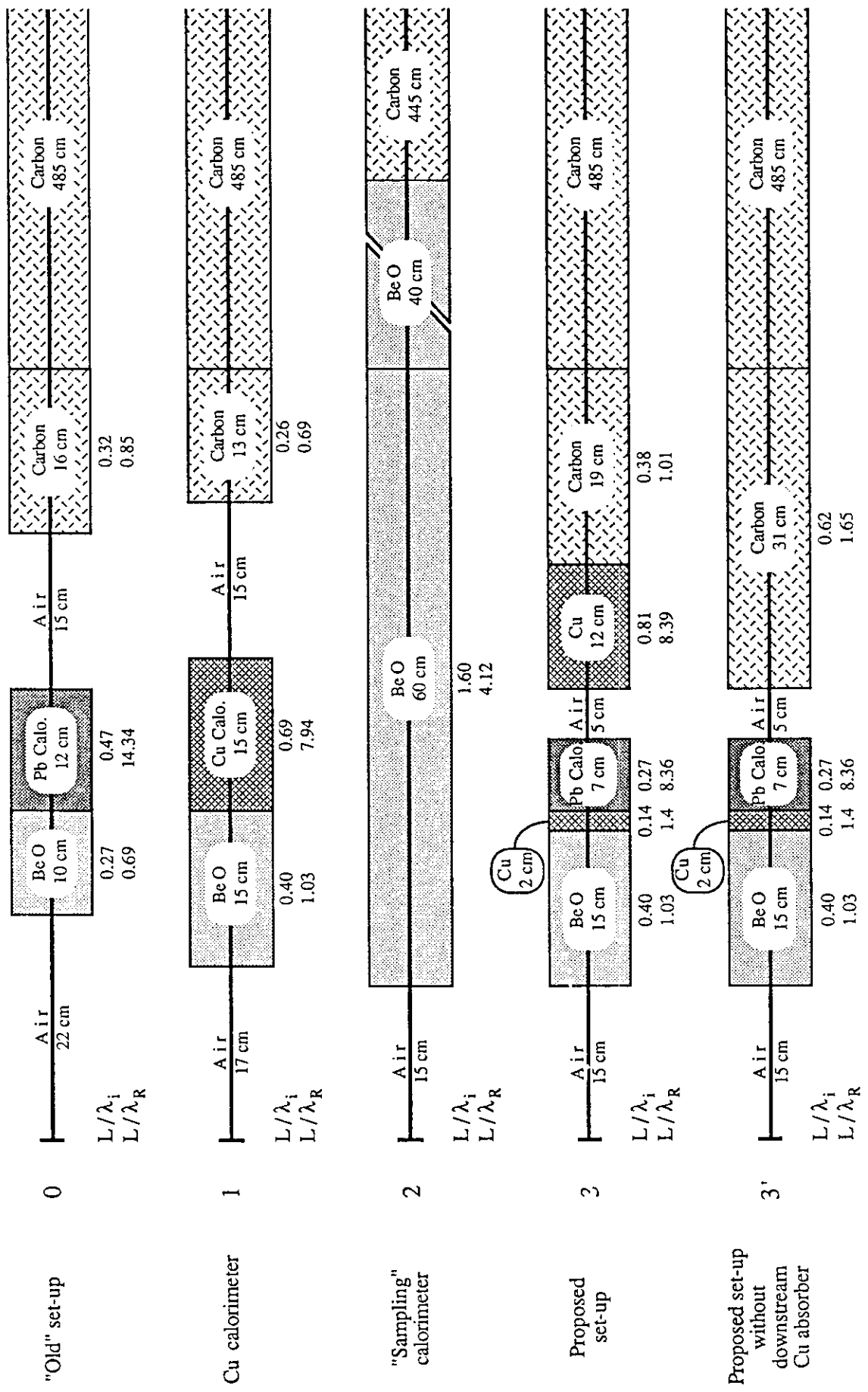


Fig. 2

Mass resolution

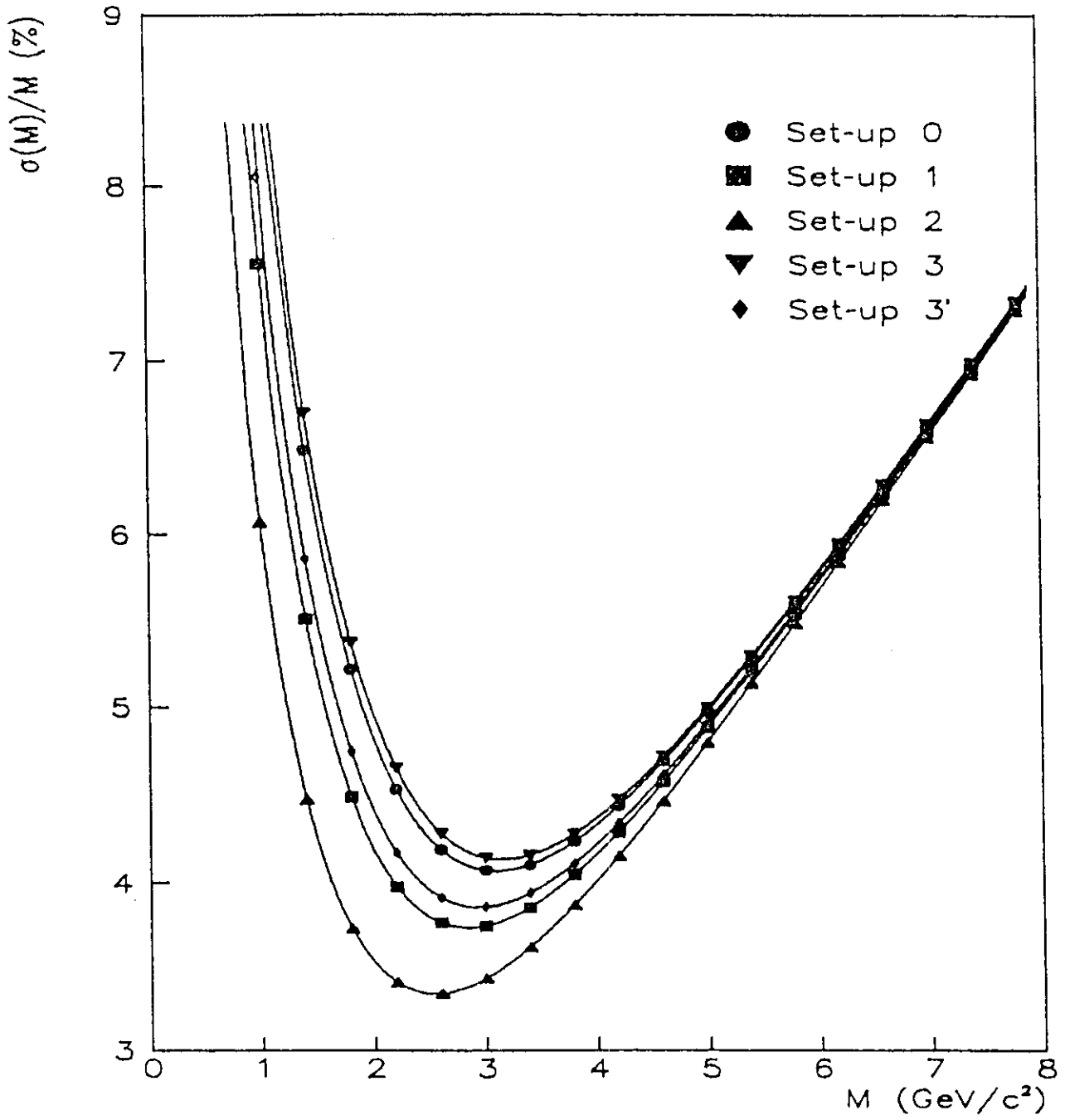


Fig. 3

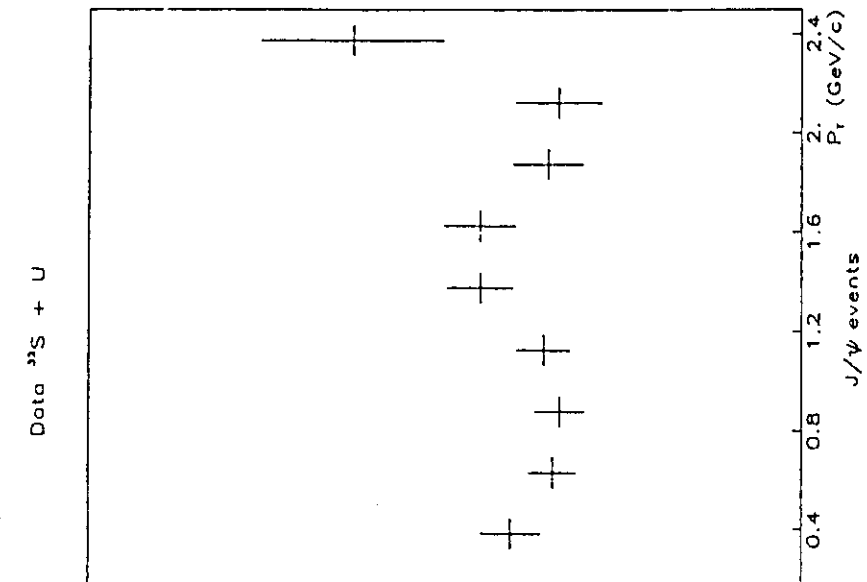
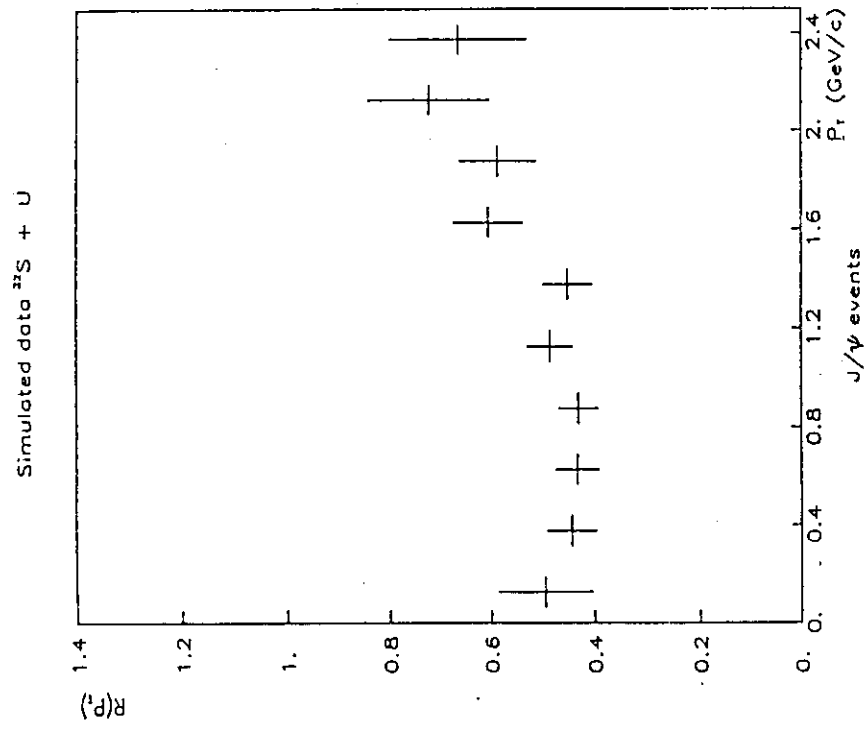
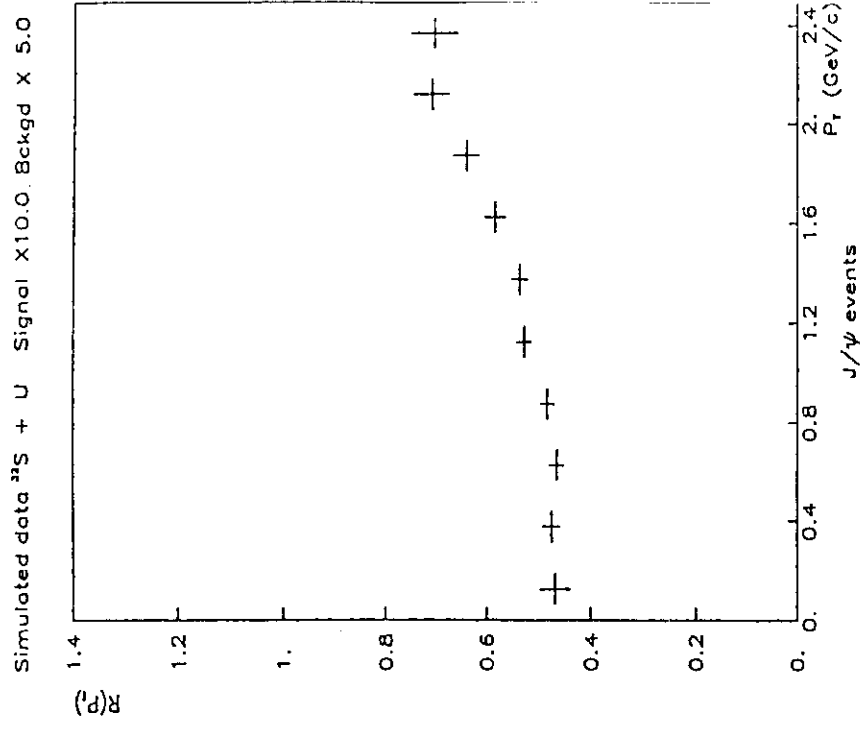


Fig. 4

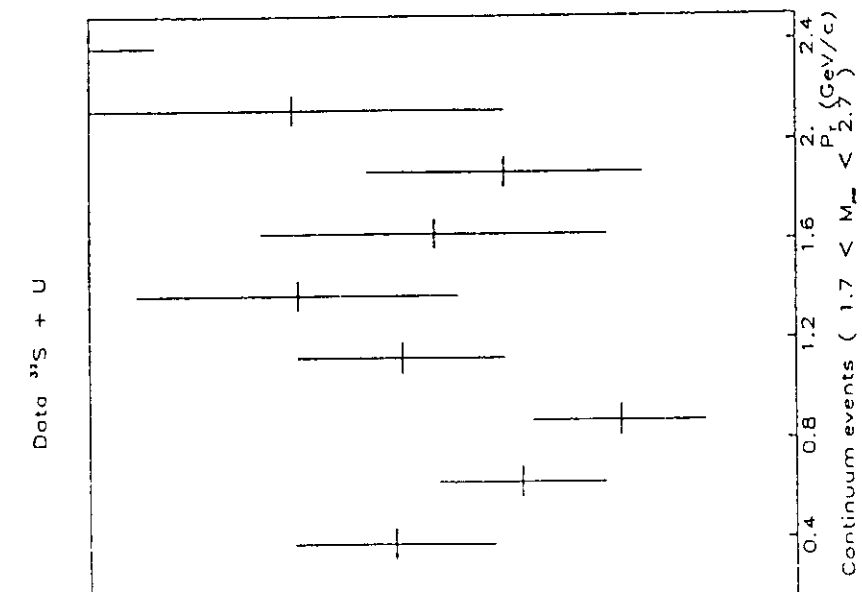
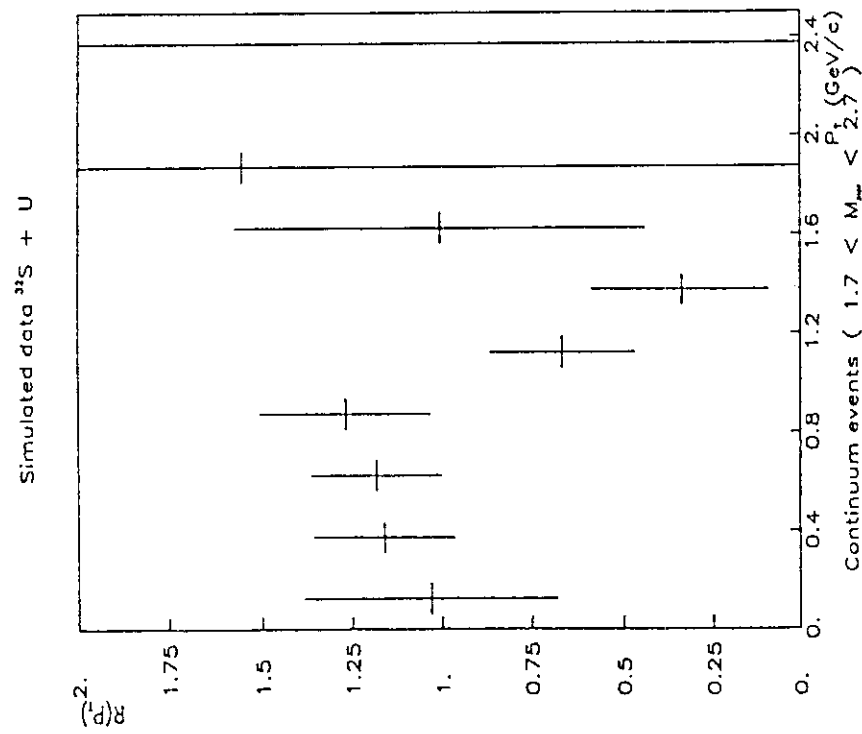
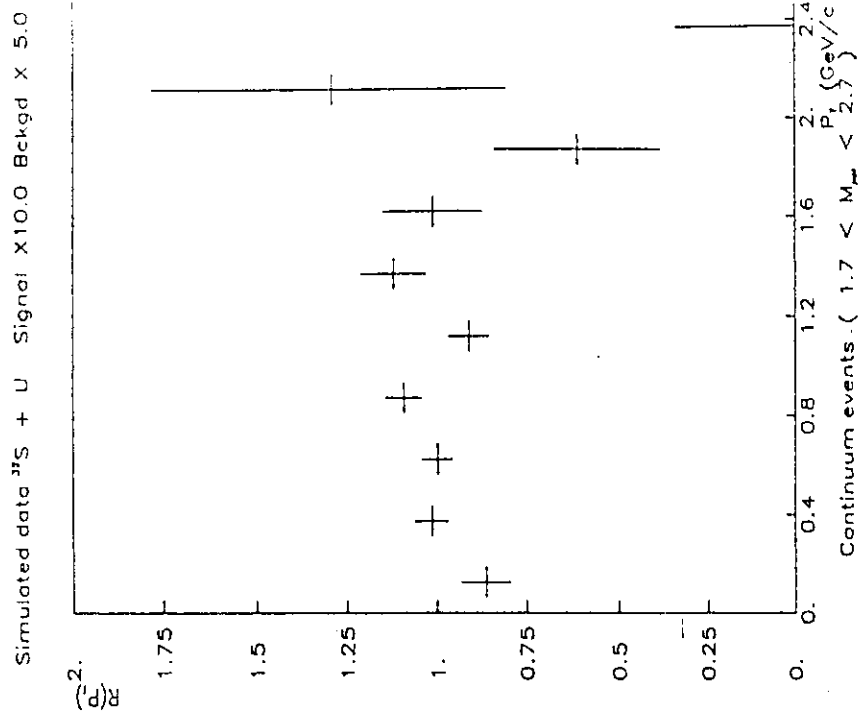


Fig. 5



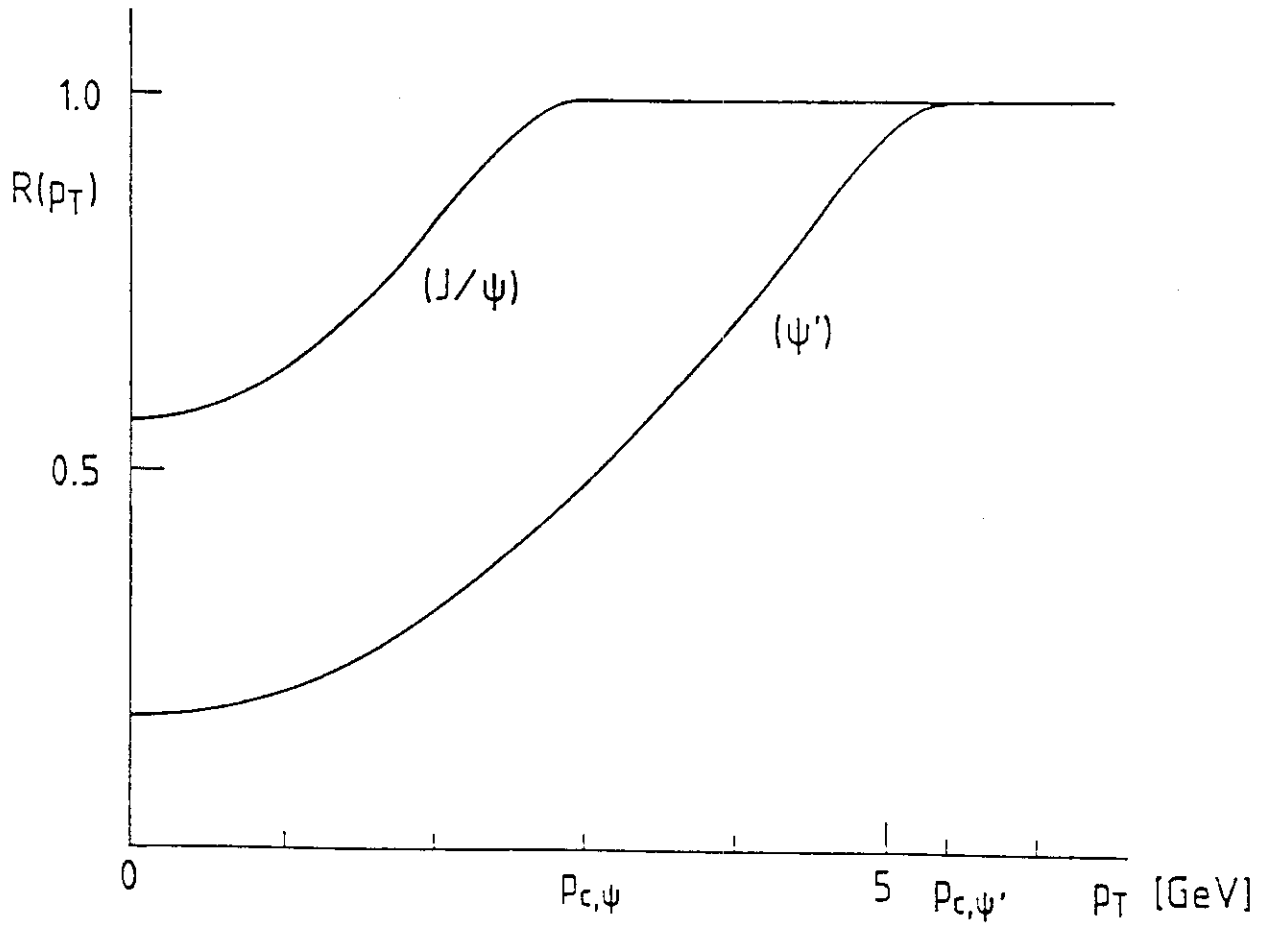
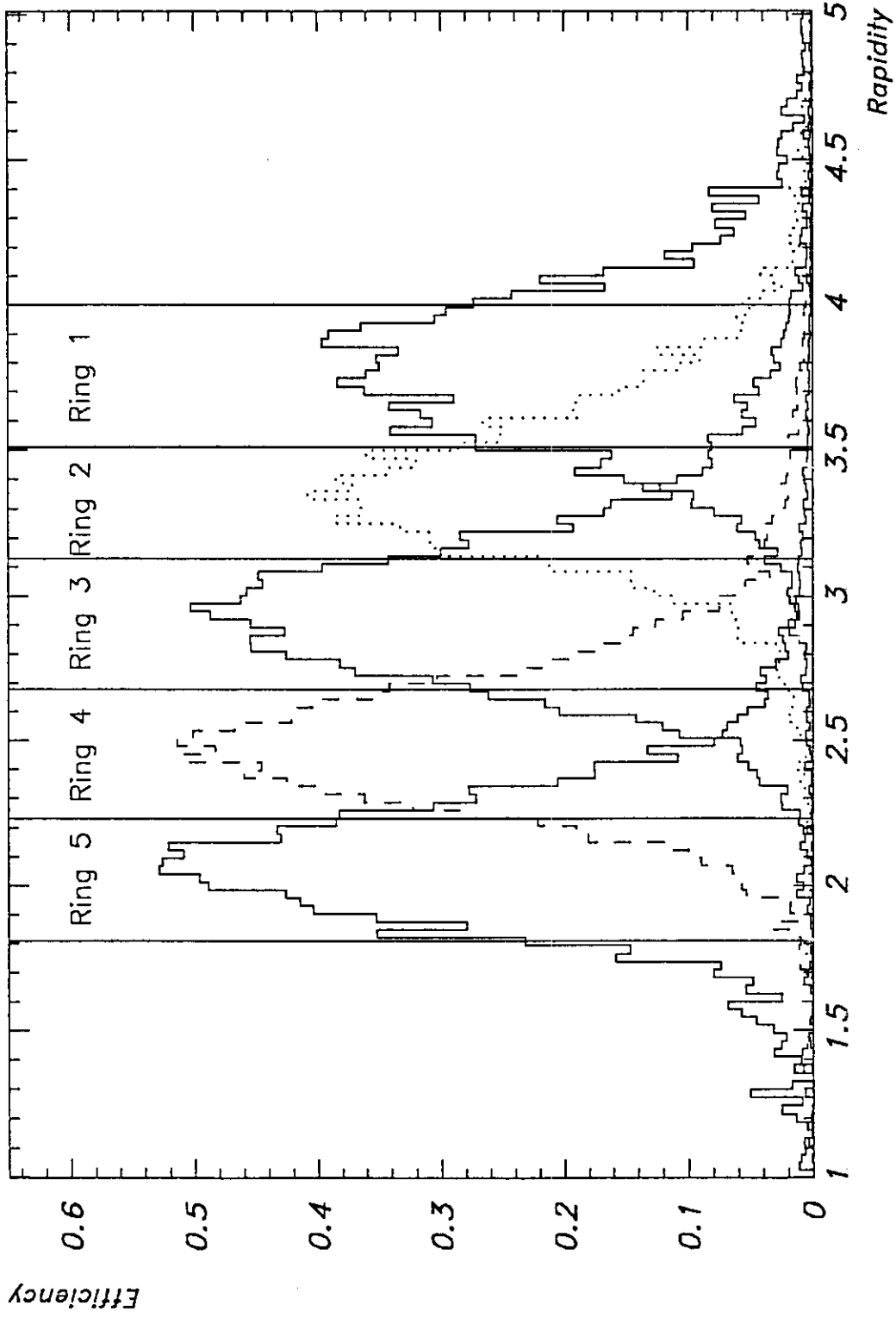
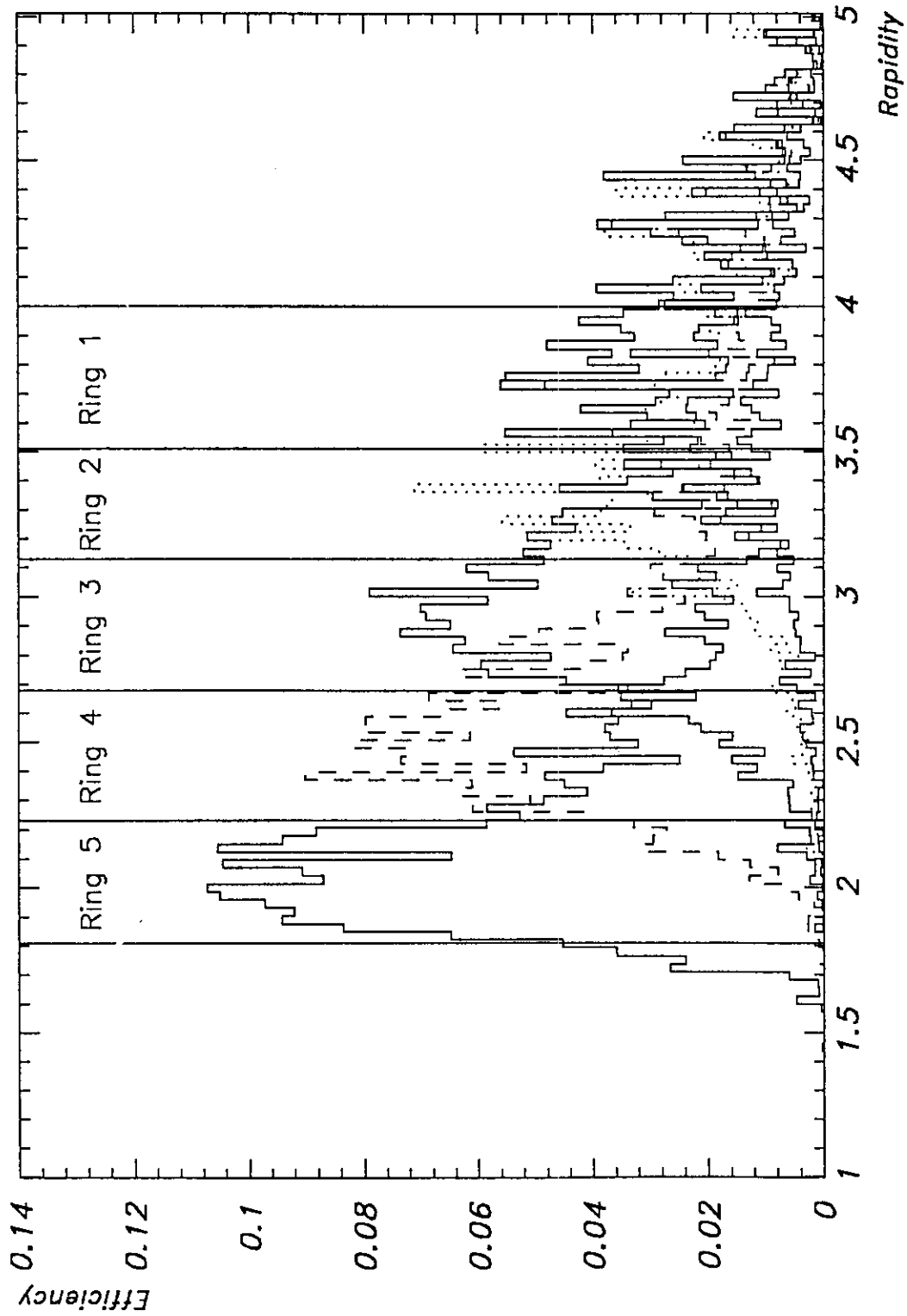


Fig. 6



Energy efficiencies of the rings

Fig. 7



*Energy efficiencies of the rings*

Fig. 8